

Effects of heat transfer and energy absorption in the ablation of biological tissues by pulsetrain-burst (>100 MHz) ultrafast laser processing

Paul Forrester,^a Kieran Bol,^a Lothar Lilge,^b and Robin Marjoribanks^a

^a Department of Physics, and Institute for Optical Sciences, University of Toronto
60 St George St., Toronto, ON M5S-1A7, Canada

^b Department of Medical Biophysics, University of Toronto,
Ontario Cancer Institute, Princess Margaret Hospital,
610 University Avenue, Rm 7-411, Toronto, Ontario, M5G 2M9, Canada

ABSTRACT

Energy absorption and heat transfer are important factors for regulating the effects of ablation of biological tissues. Heat transfer to surrounding material may be desirable when ablating hard tissue, such as teeth or bone, since melting can produce helpful material modifications. However, when ablating soft tissue it is important to minimize heat transfer to avoid damage to healthy tissue — for example, in eye refractive surgery (*e.g.*, Lasik), nanosecond pulses produce gross absorption and heating in tissue, leading to shockwaves, which kill and thin the non-replicating epithelial cells on the inside of the cornea; ultrafast pulses are recognized to reduce this effect. Using a laser system that delivers 1ps pulses in 10 μ s pulsetrains at 133MHz we have studied a range of heat- and energy-transfer effects on hard and soft tissue. We describe the ablation of tooth dentin and enamel under various conditions to determine the ablation rate and chemical changes that occur. Furthermore, we characterize the impact of pulsetrain-burst treatment of collagen-based tissue to determine more efficient methods of energy transfer to soft tissues. By studying the optical science of laser tissue interaction we hope to be able to make qualitative improvements to medical treatments using lasers.

Keywords: ultrafast laser, material processing, pulsetrain-burst, microprocessing, micromachining, dentin, enamel, laser ablation, fluence delivery, damage threshold

1. INTRODUCTION

Lasers have the potential of becoming an important tool in modern dentistry because they offer a contact-less way of modifying tissue. Vibrations and frictional heat produced by drilling machines may cause pain and discomfort to patients.^{1,2} Furthermore, laser parameters can be chosen to modify tissue in different ways — studies have demonstrated the use of lasers in ablating teeth and other hard tissue,²⁻⁶ while others have shown the potential for lasers to strengthen enamel against corrosive agents.⁶ The goal of the present study is to show that using ultrashort (≤ 1 ps) laser pulses at high repetition-rates, different types of material modification can be achieved, which gives this mode of fluence-delivery a special niche for dental surgery.

Long pulse, and short-wavelength, laser systems (≥ 10 ps pulses) interact with dental tissue through linear absorption,⁶ which leads to ablation through heating of material. This type of heating can lead to thermo-mechanical stress fractures,² and thermal diffusion causes less-precise ablation. Furthermore, efficient ablation is limited by the wavelength-dependent peak-absorption characteristics of the material. CO₂ laser systems running at 9.6 μ m⁶⁻⁸ and Er:YAG laser systems at 2.94 μ m^{6,8} are typically used for ablating dental hard tissue, which is strongly absorbing in the infrared (IR). Free-electron lasers have also been suggested as a potential tool for laser microprocessing dental hard tissue, since these systems are tunable in the IR region.⁸ The per-pulse removal rates of these systems can be high — up to 70 μ m/pulse.² However, due to heating these systems are limited to a few Hz.²

Send correspondence to: P. Forrester, E-mail: pforrest@physics.utoronto.ca, Telephone: 416 978 4400

More recently, ultrashort pulses have been investigated for use in ablating dental hard tissue. Ultrashort pulses lead to photon densities high enough to ionize material through multiphoton absorption. Once the material is ionized, free electrons absorb light through inverse Bremsstrahlung absorption and gain sufficient kinetic energy to cause further ionization through collisions, leading to the cascaded process of avalanche ionization.⁹ The combination of multiphoton absorption and avalanche ionization produces a dense plasma of free electrons in the material, which subsequently partition their energy to the ion-lattice. Ablation occurs when material is thereby sublimated or is subsequently thermally ejected from the material. For long-pulse laser-plasma interaction, the dense plasma may hydrodynamically expand during the pulse, forming a long gradient around critical electron-density in which laser energy may be efficiently absorbed; for ultrafast laser-plasma interaction, very steep pressure gradients efficiently convert the absorbed energy to directed kinetic energy of ablated material, which carries away much of the absorbed energy before much thermal diffusion to the substrate takes place.

The physical advantage of ultrashort pulses in material-processing is principally one that exploits the difference of distance-scales and time-scales — femtosecond pulse-durations are much shorter than typical thermal relaxation times of biotissues,¹ which are on the order of $1\ \mu\text{s}$ for energy deposited by absorption of $9.6\ \mu\text{m}$ laser light in dental enamel.⁶ Heat does not have time to diffuse — the hot plasma decouples, carrying away the deposited energy and leaving the rest of the sample relatively cold.

The benefit of plasma-mediated ablation is that material is *only* efficiently removed in the region where the intensities were sufficient for a plasma to form. The result is clean ablation only in the irradiated area, with little or no thermo-mechanical stress fractures and predictable ablation depths.^{1-4,10} The weakness of ablation with ultrashort pulses is that the benefit is associated with thin heated layers and steep pressure gradients; therefore ultrafast-laser etch rates are slow compared to longer pulses, only on the order of a micron per pulse,² which at low repetition rates is too slow for practical clinical use.

For clinically viable ultrashort ablation of dental hard tissue, a high repetition rate source provides an ideal solution. Our laser system delivers $1 - 10\ \mu\text{s}$ pulsetrain bursts of 1-picosecond (950fs) pulses at $\geq 100\text{MHz}$ repetition-rates, while typical amplified ultrafast laser systems run between 10 Hz–100 kHz. Unique control of fluence delivery is achieved by adjusting the per pulse energy and pulsetrain length. This permits us to separately manipulate physical processes that depend on ultrafast laser pulses and those characteristic of longer-time heat diffusion. The short amount of time (7.5 ns) between pulses means that heat from pulses of the pulsetrain accumulate, conditioning the surface for ablation; essentially, processing takes place in a material which has first been modified by warming. For processing brittle materials such as fused silica, we have previously shown we can initially produce a ductile state of the material, and the ductile material is then processed without producing shock fractures, and without leaving inbuilt stresses or cracking from thermal cycling. This leads to clean ablation with smooth features¹¹

Because the pulsetrain interacts over a long period, some heat similarly is expected to be deposited to hard biotissues. In the present study we show that the same advantages hold for ablation of dental hard tissue using an ultrashort pulsetrain burst laser system, and that by controlling the pulsetrain duration and the per-pulse energy, we can control how, and how much, the material is modified.

2. EXPERIMENTAL SETUP

2.1. Laser system

The laser used in these experiments is a flashlamp-pumped picosecond Nd:glass system ($\lambda = 1054\ \text{nm}$) purpose-built at the University of Toronto.¹² An oscillator with active-passive and feedback-controlled modelocking produces a quasi-cw pulsetrain of over 3000 pulses, with pulse duration adjustable in the range 1 – 10 ps (Figure 1). At the oscillator, intrinsic pulse energies are up to $1\ \mu\text{J}$, with interpulse separations of 7.5 ns (133 MHz). A Pockels cell N -pulse slicer selects a square burst of pulses from the train, 0.05–10 μs long, for further amplification (Figure 1, inset). Two multi-pass Nd:glass amplifiers increase the per pulse energy to up to $\sim 10\ \mu\text{J}/\text{pulse}$, giving a total train energy of up to 12 mJ in a 10 μs burst (Figure 2).

For the current studies, the beam was focused using an 8mm focal-length lens. Focal-spot imaging showed elliptical focal spots of size $4.5\ \mu\text{m} \times 6\ \mu\text{m}$. Targets were mounted on an xyz translation stage of micrometer precision. Temporal profiles and total energies of the pulsetrains were measured for the incident beam. Optimal

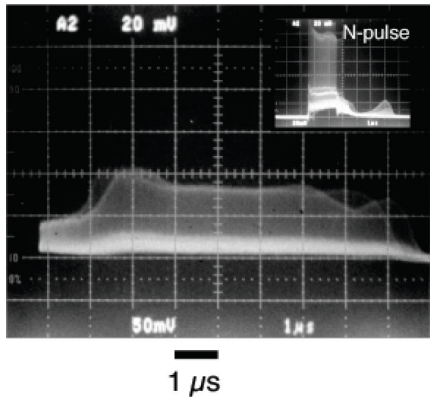


Figure 1. Oscilloscope trace of the pulsetrain-burst ultrafast-laser output: 10 – 3000 nearly equal-intensity pulses, 1 – 10 ps each, 7.5 ns between pulses (133 MHz); up to 10 $\mu\text{J}/\text{pulse}$, 15 mJ/pulsetrain-burst. An N -pulse Pockels-cell slicer controls duration of the burst (inset).

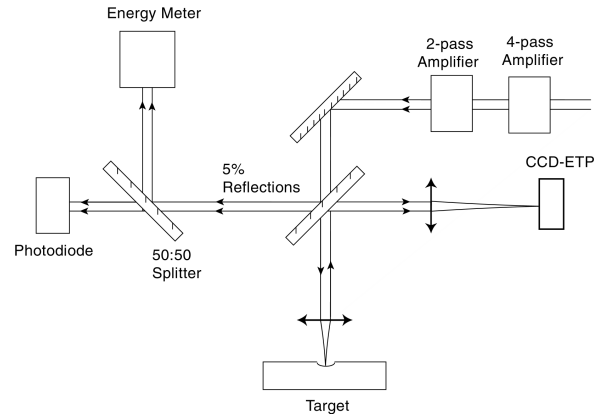


Figure 2. Experimental setup for tooth ablation. The energy per pulse and the pulsetrain duration are measured by directing the beam to an energy meter and to a fast photodiode. Focusing was determined using autocollimation and imaging to an equivalent target-plane (ETP).

focusing was regularly monitored by autocollimating the retro-reflected beam, from which an equivalent-target-plane (ETP) image was recorded on each shot (Figure 2, CCD-ETP). All shots were performed in air with the laser at normal incidence to the target.

2.2. Sample preparation

Human teeth samples were obtained from the Department of Dentistry at the University of Toronto after sterilization. Teeth were set in resin and then sectioned into 1mm slices using a diamond saw. The samples were placed on microscope slides and then laser-irradiated at normal incidence. An optical microscope (OM) was used for preliminary examination of the irradiated samples before they were coated with evaporation-deposited gold and viewed under a scanning electron microscope (SEM). Stereoscopic SEM images were taken by tilting the samples eucentrically around the ablated site at the surface plane (Figure 3, and a three dimensional digital-elevation model (DEM) (Figure 5) was created using stereoscopic *MeX* imaging software (Alicona Imaging), a post-processing analysis package for scanning electron microscopy.

2.3. 3D digital-elevation model from SEM stereoscopic imaging

A given sample was placed on a eucentric stage in the SEM, and the height adjusted so that tilting axis was at the surface of the sample, as in Figure 4. The images were brought into sharp focus so that the maximum amount of detail could be seen — detail is important because it is from the relative motion of specific features that *MeX* software reconstructs a 3D image. The stage was tilted between 2-5 degrees, making sure that the side walls did not obstruct the line of sight to the bottom of the holes — a clear line of sight is especially critical for volume analysis since any area out of view cannot be interpreted properly by the software. The tilt angle was measured by attaching a laser pointer to the eucentric stage and measuring the distance that the beam traveled as the angle increased. Using a laser pointer gave an angular resolution of ± 0.1 degree, which translates into a depth resolution of $\pm 1 \mu\text{m}$.

By creating a 3D digital-elevation model using *MeX* software, we were able to analyze the ablated sites as digital objects with the freedom to translate and rotate in a 3D environment (Figure 5). As a result we were able to study the morphology of the irradiated sites, and measure the ablated width, height and volume while keeping the sample intact. Once the DEM had been created, line-out height profiles of the 3D reconstruction were taken and the etch depths were measured from those. Figure 6 is a profile of the ablated site taken from the 3D reconstructed image.

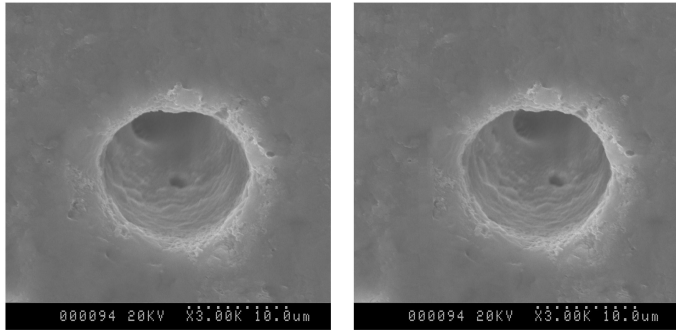


Figure 3. Stereoscopic scanning electron microscope image of human tooth irradiated by $10\mu\text{s}$ pulsetrain.

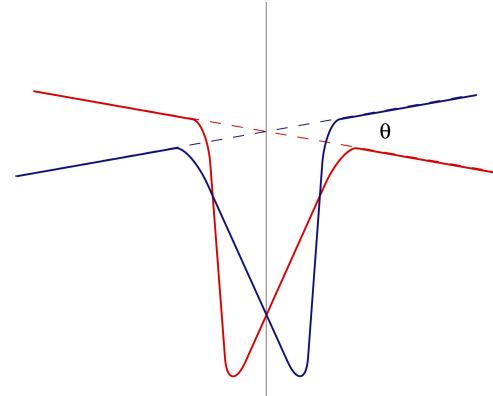


Figure 4. To create a stereoscopic image the sample must be tilted eucentrically about the surface of the sample.

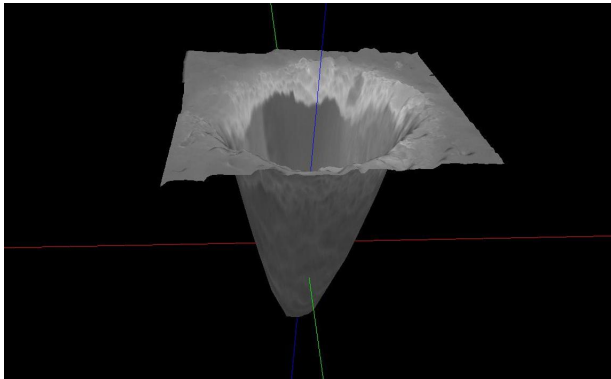


Figure 5. Three dimensional digital-elevation model created in *MeX* imaging software (Alicona) using the stereoscopic pair.

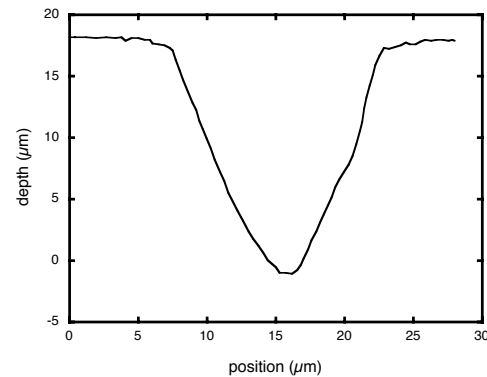


Figure 6. Profile of hole taken from 3D reconstructed image used to measure depth.

3. RESULTS

3.1. Damage threshold

Single $10\mu\text{s}$ pulsetrains of 1ps pulses, of varying total energies, were focused onto sectioned human tooth samples using an $f = 8\text{mm}$ aspherical lens (Geltech, Thorlabs Inc.). Damage was inferred by the presence of a visible spark, and later confirmed through SEM images. From these data, for multiple shots, the damage threshold for pulsetrain-bursts was found. The damage threshold for dentin was found to be approximately $1 \pm 0.5 \text{ J/cm}^2$ per 1ps pulse, within pulsetrains, which is comparable to previously published results for single pulses.²⁻⁵

3.2. Fluence delivery

3.2.1. Fluence division

The manner in which fluence is delivered to tissue directly affects how the tissue is modified. An important consequence of this is the concept of fluence division. In the past we have seen evidence in fused silica that there is a latency in the first microsecond of pulsetrain-burst interaction; even for per-pulse intensities already above threshold, there can be an effect of conditioning the interaction which affects etch-rates later in the pulsetrain. Possibly these pulses modify the material state (*e.g.*, creating ductility) or are taken up in establishing a mediating plasma in a confined geometry. This may be related, also, to our observation in metals that microprocessing can

take place for pulsetrains even when the per-pulse fluence is below the damage threshold for individual pulses. Thus, dividing the fluence-delivery into multiple bursts means investing in setting up conditions at the start of each pulsetrain-burst before deeper or more efficient processing take place.¹¹

To test this hypothesis we divided a fixed total-fluence delivery into multiple pulsetrains that added to the same number of pulses — *i.e.* 4 shots of 3 μs , 3 shots of 4 μs , 2 shots of 6 μs and 1 shot of 12 μs . The results are shown in Figure 7. Shots that were broken into multiple pulsetrains had shallower penetration depths than shots that were broken into fewer pulsetrains. Moreover, the trend is non-linear, indicating that the more broken-up the fluence delivery, the more energy went into preconditioning the tissue for ablation. This is a logical conclusion, since if each pulsetrain requires n pulses to set up a steady-state plasma, then N pulsetrains would invest $n \times N$ pulses, and concomitantly less energy was available for the second stage of etching. If the desired result is a deep etched feature, then the total fluence should be delivered in a single pulsetrain-burst; breaking the fluence delivery into several pulsetrains would be preferred in the case that the mechanism of latency produces useful material changes — for instance if absorption into low levels of heat diffusing into the material was preferred for changing the state or phase of the material being processed.

3.2.2. Material modification

The mix of timescales (pulse-duration and pulsetrain-duration) involved in pulsetrain-burst processing gives new dimensions of control of the fluence delivered to the tissue. The pulse duration is short compared to characteristic thermal diffusion timescales of materials-processing, but the pulsetrain-duration is relatively long compared to this and to hydrodynamic timescales of ablation. One aspect of these studies, therefore, is to examine the impact of pulse duration and of pulsetrain duration on micromachining and materials-processing.

Ultrafast laser pulses produce high fields, and optical breakdown in transparent media, while relatively modest fluences are delivered. At the same time, the brief pulse-duration means that little transport of heat into the material takes place during the pulse. One effect of this is that the volume of material heated is very shallow during the irradiation; once the pulse is over, the subsequent expansion, at a rate characteristic of the composition and temperature of the heated material, doubles the volume of the heated material much sooner than happens for a thicker layer heated by a long-pulse laser, and is driven by a larger pressure-gradient. As a result, the heated volume cools much more quickly, and thermally decouples from the colder substrate more rapidly, than for longer laser pulses. Consequently, the thermal imprint on the material is much reduced and clean ablation results (Figure 8 right).

Pulsetrain-burst processing affords the possibility of controlling the residual heat left in the material between pulses. Micromachining, for instance, can be modified because pulsetrain-burst processing proceeds on a material that the pulsetrain itself has modified — for instance, causing smooth melting without any cracking. Fig. 8 shows the effect of processing dentin using two kinds of pulsetrain-burst delivery: short pulsetrains of per-pulse fluences $\sim 5\times$ threshold, and long pulsetrains around $1.2\times$ the damage threshold create melting. We are currently making systematic investigations of the morphology and composition of changes we can impose using different modes of fluence-delivery.

4. CONCLUSIONS

We have studied the basic interaction physics of ultrashort pulsetrain-burst machining of dental hard tissue and shown that burst processing allows for unique control of fluence delivery and heat transfer. By tailoring the fluence delivery, we have shown that different types of material modification can be achieved. We demonstrated

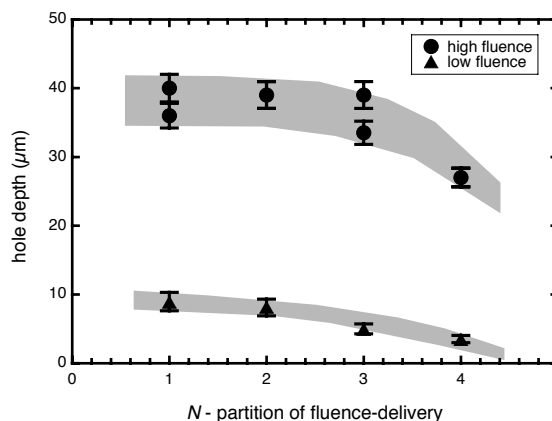


Figure 7. Overall fluence delivered to each site kept constant while number of pulsetrains that fluence is delivered in changes. (low fluence data: C. Greenhalgh, University of Toronto)

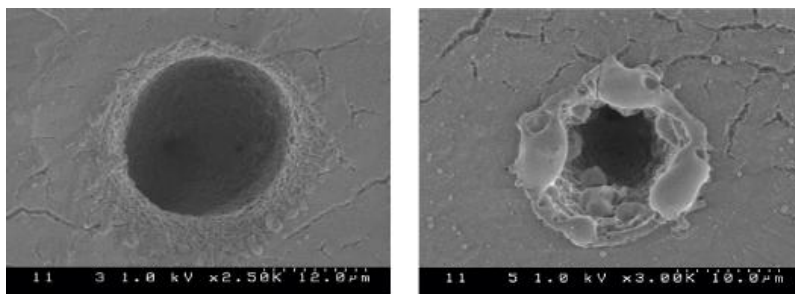


Figure 8. Clean features drilled in rat tooth (left, SEM) using short pulsetrains and per-pulse fluences well above threshold ($\sim 5\times$), while long pulsetrains around $1.2\times$ the damage threshold create melting (right, SEM).

that short intense pulsetrains result in clean ablation of tissue with very little heat deposition, while longer pulsetrains near threshold lead to smooth melted features without any thermo-mechanical fractures. Finally, we showed that the initial pulses in a pulsetrain do not contribute equally to creating deeper features — instead we hypothesize that these pulses are invested in conditioning the material in ways that change the nature of the interaction, *e.g.*, possibly establishing particular conditions of a pre-formed plasma that alters the efficiency of plasma-mediated ablation.

Pulsetrain-burst machining shows results that are promising for use in dentistry. Future studies will focus on characterizing the ablation rates of ultrashort pulsetrain-burst systems compared to conventional system operating at slower repetition rates ($\sim 1 - 100$ kHz). Also we are further studying the potential of pulsetrain-burst microprocessing for controlled material modification of hard tissues. This research will contribute to more selective and more efficient processing for medical treatments with lasers, and a better understanding of the processes involved.

5. ACKNOWLEDGEMENTS

The authors acknowledge support from the Centre for Photonics (Ontario Centres of Excellence, Inc.), the Canadian Institute for Photonic Innovations, and the Natural Sciences and Engineering Research Council of Canada. Thanks also to Dr. Johan Heershe for assistance with tooth samples.

REFERENCES

1. J. Kruger, W. Kautek, and H. Newsely *Applied Physics A* **69**, p. S403, 1999.
2. J. Neev, L. B. Da Silva, M. D. Feit, M. D. Perry, A. M. Rubenchik, and B. C. Stuart *IEEE Journal of Selected Topics in Quantum Electronics* **2**(4), pp. 790–800, 1996.
3. A. Rode, B. Luther-Davies, B. Taylor, M. Graessel, J. Dawes, A. Chan, R. M. Lowe, and P. Hannaford *Australian Dental Journal* **48**(4), p. 233, 2003.
4. B.-M. Kim, M. D. Feit, A. M. Rubenchik, E. J. Joslin, P. M. Celliers, J. Eichler, and L. B. Da Silva *Journal of Biomedical Optics* **6**(3), pp. 332–338, 2001.
5. A. Chan, A. Rode, E. Gamaly, B. Luther-Davies, B. Taylor, J. Dawes, M. Lowe, and P. Hannaford *International Congress Series* **1248**, pp. 117–119, 2003.
6. J. D. B. Featherstone and D. Fried *Medical Laser Application* **16**, pp. 181–194, 2001.
7. M. Ivanenko, M. Werner, S. Afilal, M. Klasing, and P. Hering *Medical Laser Application* **20**, pp. 13–23, 2005.
8. K. Awazu *International Congress Series* **1248**, p. 29, 2003.
9. A. Vogel and V. Venugopalan *Chemical Review* **103**(2), pp. 577–644, 2003.
10. J. Serbin, T. Bauer, C. Fallnich, A. Kasenbacher, and W. H. Arnold *Applied Surface Science* **197-198**, pp. 737–740, 2002.

11. L. McKinney, F. Frank, D. Graper, J. Dean, P. Forrester, M. Rioblanco, M. Nantel, and R. Marjoribanks **5970**, 2005.
12. R. Marjoribanks, F. W. Budnik, G. K. L. Zhao, M. Stanier, and J. Mihaychuck *Optics Letters* **18**, pp. 361–363, 1993.